Fault location in electrical distribution systems using PLS and NN

M.L. Ruiz [1], J. Meléndez [1], J. Colomer [1], J. Sánchez [2] and M. Castro [2]

[1] Group Engineering of Control and Intelligent Systems (eXiT)
University of Girona, Spain,
e-mail : (mlruizo,quimmel,colomer)@eia.udg.es

[2] ENDESA, Spain
e-mail: jslosada@fecsa.es, MCastro@enher.es

Abstract. This paper discusses about voltage sags fault location using a temporal and phasorial descriptors. A dimensionality reduction technique is used to extract the significant features from voltage sags descriptors and a Neural Network is applied to locate the fault.

Key words

Voltage sags, PLS, NN, Fault detection.

1. Introduction

The concept *power quality* has received more importance by new regulation in the electrical sector. It has become a very important reason to encourage researches in fault location. The fault origin can be due to: the electrical facility operation, operation of specific non-linear loads, short circuits, among others. These faults are usually transmitted to the whole electrical system. Responsibility of possible damages caused to customers is assigned to utilities [1]. Consequently, the utilities are interested in monitoring (characterizing, recognizing, location) of these perturbations.

The voltage sags are registered fault in a 25kV Spain Electrical Facility. In this work, the goal is to locate faults based on temporal [6] and phasorial descriptors [9]. Descriptors used are; four temporal and three phasorial descriptors. Temporal descriptors are: (1) three phase sag magnitude, (2) three phase sag duration, (3) starting time and (4) ending time[6] (see figure 1). Phasorial descriptors are (1) the minimum, (2) the maximum and (3) the average PNfactor where PNfactor is the difference between positive-sequence and negative-sequence [9].

The voltage sags location can be either distribution or transmision voltage level [5]. Partial Least Squares (PLS) and Neural Network (NN) are used as solution tools. PLS is a dimensionality reduction technique. It is used to extract significant features from voltage sags descriptors. Then, NN are applied to locate the origin of the fault.

This paper is organized as follow. Sag attributes are presented in section 2. In sections 3 and 4, two tools (PLS and NN) are presented to solve the problem. In section 5, a numerical example is developed using voltage sags recorded in 25kV facility during one year period. Finally, conclusions and acknowledgments are in sections 6 and 7.

2. Definition of Significant Voltage Sag Descriptors

Voltage sags have been characterized in this work by using temporal and phasorial descriptors. Temporal descriptors are obtained from measurements of the duration and magnitude. The phasorial descriptors are represented qualitatively according to the method presented in [9].

A. Temporal descriptors

Temporal descriptors depicted in figure 1 are [9]:

1) *Three-phase sag magnitude (H)*: It is defined as the maximum drop of voltage of three-phase power system during the sag.
2) *Three-phase sag duration (TDH)*: It is defined as the maximum time during the rms voltage in the three phase power system, is lower to 0.9p.u.
3) *Starting time (TIH)*: It is defined as the moment immediately the rms voltage in the three phase power system, lower of 0.9p.u.
4) *Ending time (TFH)*: It is defined as the moment immediately the rms voltage in the three phase power system, recuperate to 0.9p.u.

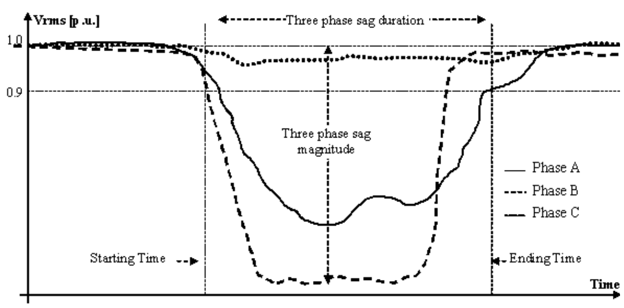

Fig. 1. Temporal descriptors in voltage sags

B. Phasorial descriptors

A technique proposed in [9] to characterize sags, has been applied, which enables a characterization through one complex voltage, without significant loss of information. The method is based on the decomposition of the voltage phasors in symmetrical components. Positive-sequence voltage $\vec{V}_1$, negative-sequence voltage $\vec{V}_2$ and zero-sequence voltage $\vec{V}_0$ are calculated from the complex phase voltages $\vec{V}_a$, $\vec{V}_b$ and $\vec{V}_c$ as follows:

$$\begin{pmatrix} \vec{V_0} \\ \vec{V_1} \\ \vec{V_2} \end{pmatrix} = \frac{1}{3} \begin{pmatrix} 1 & 1 & 1 \\ 1 & a & a^2 \\ 1 & a^2 & a \end{pmatrix}$$

where

$$a = -\frac{1}{2} + \frac{1}{2} j\sqrt{3} \tag{1}$$

The voltage sag type indicates which phases are involved in the event. The seven basic types are given in figure 2. Balanced voltage sag (type *A*) is due to an equal drop in the values of voltage in the three-phases. Unbalanced voltage sags (types *C* and *D*) depend on the phases involved. The *C*-types are voltage drops between two phases: type *Ca* is a voltage drop between phases *b* and *c*, type *Cb* between phases *a* and *c*, and type *Cc* between phases *a* and *b*. The *D*-types are voltage drops in one phase: type *Da* is a voltage drop in phase a, type *D*b in phase *b*, and type *Dc* in phase *c*.

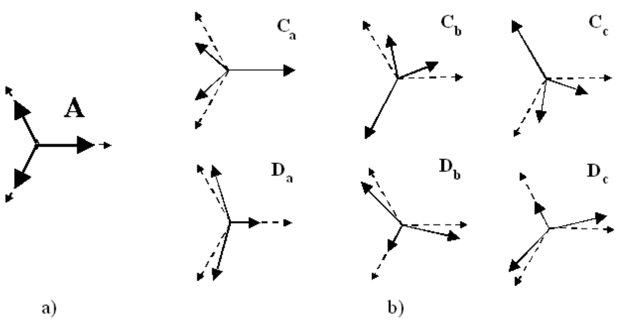

Fig. 2. a) Three-phase balance voltage sag, b) six types of three-phase unbalanced voltage sags

The voltage sag type is found from the angle between positive-sequence voltage $\vec{V}_1$ and negative-sequence voltage $\vec{V}_2$. The classification method is described in more detail in [1] and summarised as follows:

$$k = round\left(\frac{angle(\overrightarrow{V_2}, 1 - \overrightarrow{V_1})}{60^o} \right)$$

where,

k=0: type Ca	k=1: type Dc	k=2: type Cb
k=3: type Da	k=4: type Cc	k=5: type Db

Knowing the voltage sag type, the negative-sequence voltage can be calculated back to the corresponding value for prototype voltage sag:

$$\vec{V_2}' = \vec{V_2} e^{-jk60^o} \tag{2}$$

PN-factor $\vec{F}$ is obtained from:

$$\vec{F} = \vec{V_1} + \vec{V_2}' \tag{3}$$

The proposal is to use PN-factor average, PN-factor minimum and PN-factor maximum to characterize three-phase unbalanced voltage sags. In table I are showing some events with our temporal descriptors and fasorial descriptors.

TABLE I. - Voltage sags descriptors

File	TIH(mS)	TFH(mS)	TDH(mS)	H	PNF min	PNF max	PNF average
SALT_04-05-2002_14_22_34	46,8960	147,2534	100,3574	22,6832	0,9132	0,9812	0,9397
SALT_04-05-2002_15_57_33	85,9760	270,4336	184,4576	23,4902	1,0022	1,0281	1,0151
SALT_08-05-2002_16_00_10	47,8339	214,1584	166,3245	22,8993	0,7827	1,0352	0,8747
SALT_11-04-2002_20_31_01	86,2886	246,6730	160,3843	20,8889	0,7935	1,0123	0,8439
SALT_12-07-2002_15_50_13	81,5990	182,5818	100,9827	27,5412	0,7439	0,9880	0,8313

3. Partial Least Squares (PLS)

A. Brief introduction

PLS, also known as *Projection to Latent Structures*, it is a dimensionality reduction technique maximizing the covariance between the predictor matrix *X* and the predicted matrix *Y* for each component of the space. The predictor is let the data in training set, consisting of *m* variables and *n* samples for each variable [7], in this research the predictor matrix *X* has 7 and 100 different events by each variable. This information is stacked into a matrix $X \in R^{7x100}$ given by:

$$X = \begin{array}{c} \begin{array}{ccccccc} TIH & TFH & TDH & H & PNF_{min} & PNF_{max} & PNF_{ave} \end{array} \\ \begin{bmatrix} 46.896 & 147.25 & 100.36 & 22.683 & 0.9132 & 0.9812 & 0.9397 \\ 85.976 & 270.43 & 184.46 & 23.49 & 1.0022 & 1.0281 & 1.0151 \\ 47.834 & 214.16 & 166.32 & 22.899 & 0.7827 & 1.0352 & 0.8747 \\ . & . & . & . & . & & . \\ . & . & . & . & . & ... & . \\ . & . & . & . & . & & . \\ 50.625 & 177.81 & 127.19 & 46.27 & 1.0017 & 1.0255 & 1.0077 \\ 49.375 & 82.656 & 33.281 & 10.708 & 0.9462 & 0.9849 & 0.9701 \end{bmatrix} \end{array} \begin{array}{c} \\ 1 \\ 2 \\ 3 \\ . \\ . \\ . \\ 99 \\ 100 \end{array}$$

The predicted matrix contains the fault location, $Y \in R^{1x100}$, where 1 denoted fault in distribution and 0 represent transmission fault.

PLS computes loading and score vectors that are correlated with the predicted block while describing a large amount of the variation in the predictor matrix. PLS require calibration and prediction steps. The most popular algorithm used is PLS to compute the parameters in the calibration step is know as **Non-Iterative Partial Least Squares (NIPALS)** [7][8].

To effectively extract the information in the data relevant to process monitoring, it is often necessary to pretreat the data in the training set. The pretreatment procedures consist of autoscaling. Autoscaling standardizes the process variables (see table II). It assures a similar influence of each descriptor when dimensionality reduction technique is applied [7].

TABLE II. - Autoscaling descriptors

File	TIH(mS)	TFH(mS)	TDH(mS)	H	PNF min	PNF max	PNF average
SALT_04-05-2002_14_22_34	0.061591	0.037777	0.029904	0.053463	0.098853	0.096665	0.098807
SALT_04-05-2002_15_57_33	0.11292	0.069379	0.054963	0.055365	0.10849	0.10129	0.10673
SALT_08-05-2002_16_00_10	0.062823	0.054942	0.04956	0.053972	0.084727	0.10198	0.091972
SALT_11-04-2002_20_31_01	0.11333	0.063283	0.04779	0.049234	0.085896	0.099729	0.088733
SALT_12-07-2002_15_50_13	0.10717	0.046841	0.03009	0.064913	0.080527	0.097335	0.087409

The goal of PLS is to determinate the loading and score vectors which are correlated with *Y* while describing a large amount of the variation in *X*. This is achieved by decomposing *X* and *Y* into a combination of loadings *P* and *Q* (these are determinate of orthogonal vectors), scores *T* (it is the projections of the loading vectors associated with the first singular values), weights *W* and residual matrices *E* and *F* such that [8].

$$X = TP^T + E \tag{4}$$

$$Y = TQ^T + F \tag{5}$$

The matrix product TP^T can be expressed as the sum of the product of the score vectors t_j (the j^{th} column of *T*) and loading vectors p_j (the j^{th} column of *P*), similarly, *Y* is decomposed as the sum of the product of the score vectors t_j (the j^{th} column of *T*) and loading vectors q_j (the j^{th} column of *Q*) [7].

$$X = \sum_{j=1}^{N} t_j p_j^T + E \tag{6}$$

$$Y = \sum_{j=1}^{N} t_j q^{T_j} + F \tag{7}$$

where *N* is the number of principal components deemed to be significant. It is possible to make a model of voltage sags with *Q*-statistic and *D*-statistic. The *Q*-statistic is a measure of the lack of fit with the established model. The value for this model is 0.0104. It is defined as follows:

$$Q = \sum_{i=N+1}^{m} t_i t_i^T \tag{8}$$

where *m* is the number of process variables (descriptors) [4]. *Q* indicates the distance between the actual values of the event and the projected values onto reduced space.

The Hotelling T^2 or *D*-statistic statistic, measures the degree to which data fit the calibration model:

$$T^2 = \sum_{i=1}^{N} t_i \sigma^{-1} t_i^T \tag{9}$$

where $\sigma = 0.5021$ is the standard deviation. The value for this model is 0.0104. The *D*-statistic gives a measure of the Mahalanobis distance in the reduced space between of event and the origin that designates the point with average event.

Normally, *Q*-statistic is much more sensitive than T^2. This is because *Q* is very small and therefore any mirror change in the system characteristics will be observable. T^2 has great variance and therefore requires a great change in the system characteristic for it to be detectable.

Two principal components which explained 95.27% of the total variability in block *X* and 65.51% of variability of block *Y* (see table III).

TABLE III. - Principal component extraction

Percent Variance Captured by Regression Model

	---X-Block-----		---Y-Block----	
LV #	This LV	Total	This LV	Total
1	84.42	84.42	61.09	61.09
2	10.85	95.27	4.42	65.51

B. Detection of "non-voltage sags"

The charts *Q*-statistic and *D*-statistic contain all the information required to identify voltage sags. Figure 3 show that some event exceeds its limits. Different events were detected. These events are: interruption, overvoltage, and not fault recovery. In table IV are presented the events that exceed limits. The events were subtract for new model of voltage sags.

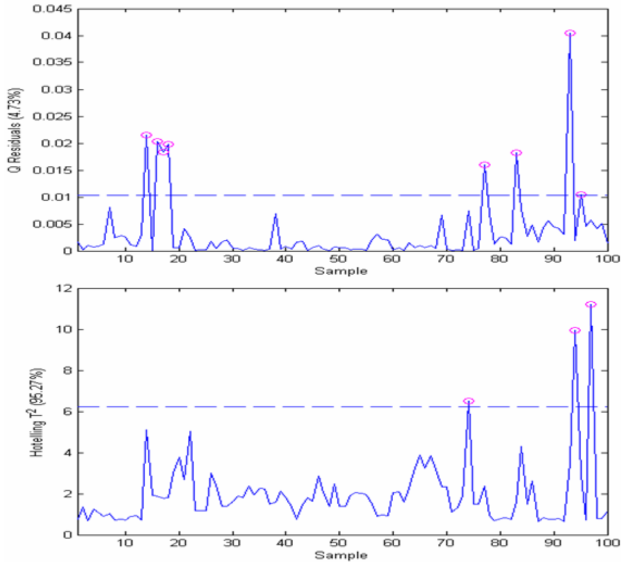

Fig. 3. Q-statistic and D-statistic with 95.27% confidence limits

TABLE IV. - Events exceeding limits a)*Q*-statistic b)*D*-statistic

Sample	File	Remark
14	Salt 17-07-2002_10-26-41	interruption
16	Salt 22-10-2002_13-37-50	It does not fault recovery
17	Salt 22-10-2002_13-41-11	It does not fault recovery
18	Salt 22-10-2002_13-53-13	It does not fault recovery
77	Acebsa 10-12-2002_18-55-28	It does not fault recovery
83	Salt_TRI 31-1-2003_15-36-59	overvoltage
93	Salt_tr35 14-02-2003_21-23-56	interruption
95	Salt_tr35 19-02-2003_13-26-52	interruption

a)

Sample	File	Remark
74	Salt 16-12-2002_09-54-00	interruption
94	Salt_tr35 19-02-2003 13-21-24	interruption
97	Salt_tr35 21-02-2003_23-23-11	interruption

b)

4. Neural Network (NN)

A. Overview

NN have been extensively used in continuous speech recognition and synthesis, image processing and coding, pattern recognition, among others. In this work a feedforward NN has been used to classify voltage sags according to is location (distribution or transmission). The classical backpropagation algorithm has been used in the learning step [2]. The input and the corresponding target was used to train the network. The input matrix can is: descriptors (see table I) or principal components (table V shows some values). Finally, the target matrix is composing by 0 and 1, where 1 denote fault in distribution and 0 represent transmission fault.

TABLE V. - Voltage sags Principal components

File	1ª PC	2ª PC
SALT_04-05-2002_14_22_34	0.19217	-0.040608
SALT_04-05-2002_15_57_33	0.24498	-0.061717
SALT_08-05-2002_16_00_10	0.20373	-0.023089
SALT_11-04-2002_20_31_01	0.21972	-0.065215
SALT_12-07-2002_15_50_13	0.20539	-0.063861

B. Architecture

This section presents the architecture of the network used with the backpropagation algorithm for fault location.

1) *First architecture:* The 7 descriptors are the input to the NN (see figure 4). The network can have several layers. First layer has *R* inputs (7), weight matrices connected to inputs, *inputsweight* (*IW*) and a bias vector *b*. Other layers have a weight matrices coming from layer outputs, *layersweight* (*LW*) and also, a bias vector *b*. The sum of the weighted and the bias forms the input to the transfer function *f*. In this work *tansig* and *logsig* function have been used to generate output vector *a*. *tansig* for first layer and hidden layer and *logsig* for output layer, because these functions are capable of approximating any function with a finite number of discontinuities [2][3].

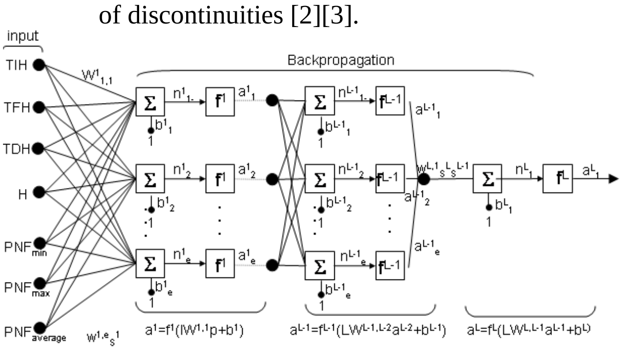

Fig. 4. First architecture

2) *Second architecture:* From 7 descriptors previously described, 2 Principal Component (PC) are obtained using the dimensional reduction technique by PLS. These PC are the input to the NN. Statistical process has a similar behaviour to NN. Descriptors matrix $X \in R^{7x100}$ and voltage sags location $Y \in R^{1x100}$ are the input to statistical phase. The objective in statistical phase is to reconstruct a lower dimension; this is optimizing the relation between matrix *X* and matrix *Y*. The optimization is based on minimization of the mean square error [2][7].

B. Backpropagation learning algorithm

The simplest implementation of backpropagation learning updates the network weights and biases in the direction in which the performance function decreases most rapidly (gradient descent). One iteration of this algorithm can be written:

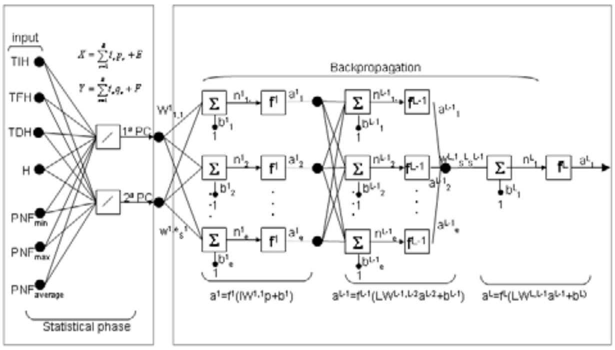

Fig. 5. Second architecture

$$w_{k+1} = w_k - \alpha_k g_k \tag{6}$$

$$b_{k+1} = b_k - \alpha_k g_k \tag{7}$$

where x_k is a vector of current weights and biases, g_k is the current gradient and $\alpha_k = 0.05$ is the learning rate. The current gradient is scaled conjugate gradient algorithm was designed to avoid the time consuming [3]. A feasibility study has been done to determinate the topology of architecture. This study is presented in next section.

5. Results and Discussion

A. Reconstruct a lower dimension with PLS

Spanish Electrical Facility (Endesa Distribution SL) has provided voltage sags in a 25kV distribution facility. 100 voltage sags were recorded but 11 were subtract because they is not voltage sags. Therefore, 89 events are used for location fault. With this change, the total variability is increase. The attributes depicted in table VI are the new principal components with its variability.

TABLE VI. - The new principal characteristic extraction

Percent Variance Captured by Regression Model

	---X-Block-----		---Y-Block----	
LV #	This LV	Total	This LV	Total
---	----	----	-----	-----
1	85.54	85.54	60.71	60.71
2	10.95	96.49	5.71	66.42

A new model of voltage sags is developed. Now, model is more adjusted (see figure 6). The new *Q*-statistic and T^2 are: *Q=0.0086*, *D=6.2738*. Figure 6 shows that some event exceeds the limits again, table VII are illustrating faults which are out of new limits. However, these events were not eliminated because they are voltage sags.

TABLE VII. - Voltage sags are out new limits
a) *Q*-statistic b) *D*-statistic

Sample	File	Remark	Waveform
14	Salt 22-10-2002_13_53_13	A long voltage sag duration	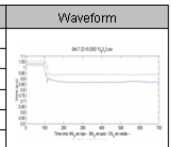
34	Salt 09-10-2002_02_23_22	A long voltage sag duration	
65	Salt 10-12-2002_18_56_12	A long voltage sag duration	
71	Acebsa1 10-12-2002_18_55_28	A long voltage sag duration	
78	Salt_TRI 31-1-2003_15-36-59	A long voltage sag duration	
85	Salt_tr35 19-02-2003_13-26-52	A long voltage sag duration	
69	Salt 16-12-2002_09_54_00	Voltage sag and Interruption	See b)

a)

Sample	File	Remark	Waveform
69	Salt 16-12-2002_09_54_00	Voltage sag and Interruption	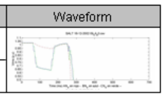
86	Salt_tr35 21-02-2003_23_23_11	Voltage sag Interruption	

b)

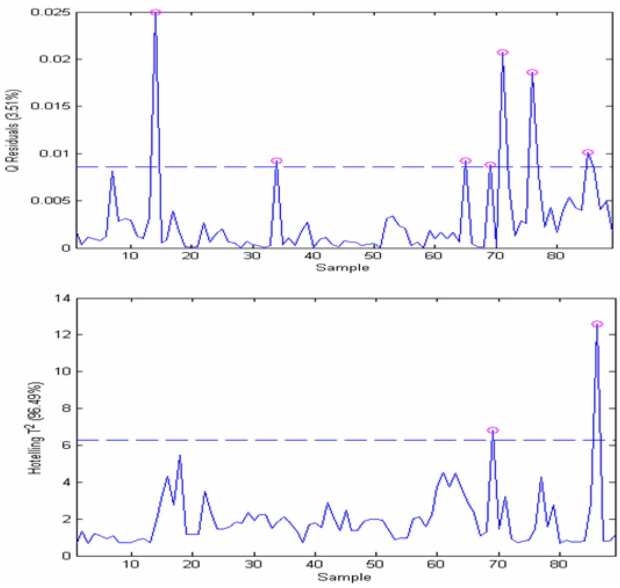

Fig. 6. New model of voltage sags

B. Fault location with NN

Feasibility Study: Applying NN to locate the origin of the fault, it is necessary to do a topology feasibility study. Different topologies were tested: 2, 3 and 4 layers and diverse number layers neurons (see figure 7 and figure 8). These figures show the error according the number of neurons by layer. Topology selected is 4 layer and 8 neurons by layer because it is smallest error. Although, the error in the first architecture is lower than second architecture, the second is best because in proportion as the number of neurons for layer grows, the error decrease.

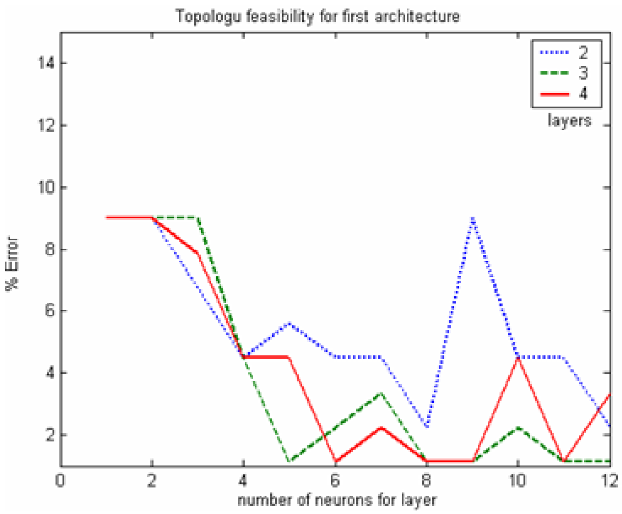

Fig. 7. Topology feasibility study of first architecture

The figure 9 shows the error according the epochs training. The error in the first architecture decrease quickly. The error in the second architecture decrease slowly but the final error is lower.

Classification: Finally, the classification has been obtained. The real location is: 45 voltage sags of distribution and 44 of transmission. Both architectures only have one error (see table VIII), but the first architecture has been benefited with statistical phase because 11 events are different to voltage sags.

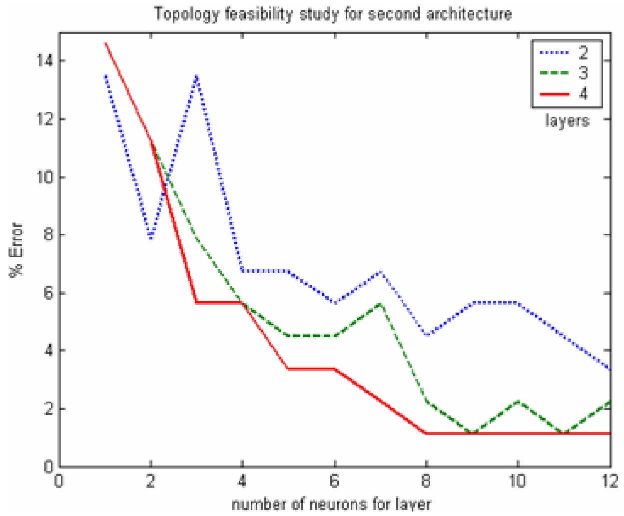

Fig. 8. Topology feasibility study of second architecture

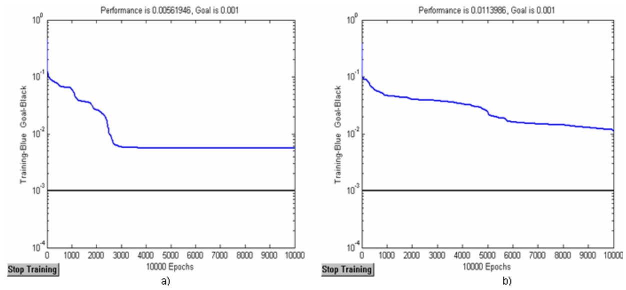
Fig. 9. a)First architecture b)Second architecture

TABLE VIII. – Voltage level classification

	Fault location		
voltage level	real	first architecture	second architecture
distribution	45	44	46
transmission	44	45	43

6. Conclusion

It is interesting to see that the PLS was able to detect 11 events different to voltage sags. Determination of voltage sags location has been performed thus the restoration become very quickly. The electrical facility gains with this information which helps companies in network normal operation to maintain the continuity indexes. It is due to the improvement on the response applying restoration strategies to recover the faulted system. Planning purpose, the information obtained by means of this analysis, will be useful to network companies to locate the zones influenced by voltage sags. It addresses the location of new sag sensitive equipment.

Acknowledgments

This work has partially been supported by Spanish government and FEDER funds, within the project (SECSE, DPI2001-2198) and a contract between UdG and Endesa Distribution SAU.

References

[1] Math H. J. Bollen. *Undertanding Power Quality Problems*. 0-7803-1713-7. Power Engineering, 2000.

[2] N.K. Bose and P. Liang. *Neural Network fundamentals with graphs, algorithms, and applications*. ISBN 0-07-006618-3. 1996, 1996.

[3] Howard Demuth and Mark Beale. *Neural Network Toolbox for Use with MATLAB*. The MathWorks, Inc, 3 Apple Hill Drive Natick, MA 01760-2098, version 4 edition, sep 2000.

[4] Barry Lennox. Multivariate statical process control. 2003.

[5] J. Melendez, J. Mora, D. Llanos, M. Ruiz, J. Colomer, J. Sanchez, and X. Corbella, editors. *Classification of short duration faults (voltages sags) in transmission and distribution power systems*. ECC European Control Conference, sep 2003.

[6] J. Mora, D. Llanos, J. Melendez, J. Colomer, J. Sanchez, and X. Corbella, editors. *Classification of Sags Measured in a Distribuiton SubstationBased on Qualitative and Temporal Descriptors*. CIRED 17th International Conference on Electricity Distribuiton, mai 2003.

[7] Evan L. Russell, Leo H. Chiang, and Richard D. Braatz. *Data Driven Techniques for Fault Detection and Diagnosis in Chemical Processes "Advances in Industrial Control"*. ISBN 1-85233-258-1, London, 2000.

[8] Barry M. Wise, Neal B. Gallagher, Rasmus Bro, and Jeremy M. Shaver. *PLS Toolbox 3 0*. Eigen Vector Research Incorporated, may 2003.

[9] L.D. Zhang and M.H.J. Bollen. A method for characterizing unbalanced voltage dips (sags) with symmetrical components. *IEEE power Engineering Letters*, jul 1998.